EUROPEAN ORGANIZATION FOR NUCLEAR RESEARCH

NP Internal Report 64-17

ABSOLUTE MEASUREMENTS OF PROTON-PROTON SMALL-ANGLE ELASTIC SCATTERING AND TOTAL CROSS SECTIONS AT 10, 19 AND 26 GeV/c

G. Bellettini, G. Cocconi, A.N. Diddens, E. Lillethun[†], J. Pahl[††], J.P. Scanlon[*], J. Walters[**], A.M. Wetherell and P. Zanella

Geneva - 14 December, 1964

10031

Previous measurements of elastic p-p scattering at GeV energies have suggested that the behaviour of the angular distribution is not exactly that expected for diffraction scattering arising from a pure imaginary scattering amplitude without spin dependence [1]. This has been maintained, experimentally, because of an excess of cross section at small angles above the value given by the optical theorem for pure diffraction scattering. No firm conclusion could be reached, however, because of various experimental difficulties, such as background, normalization problems, poor angular and momentum resolution or lack of counting statistics. The aim of the present experiment was to minimize these experimental effects and to study, in detail, the range of very small angles, extending into the Coulomb scattering region, where interference with a real nuclear amplitude would be important.

The differential cross sections for elastic proton-proton scattering at laboratory angles between about 2 and 20 mrad and for proton momenta of 10.1, 19.3 and 26.4 GeV/c were measured using thin-plate sonic spark chambers in an arrangement of magnetic spectrometers. Subsidiary scintillation counter experiments with the same geometries gave the p-p total cross sections at the three proton momenta used. Substantial deviations above the optical theorem value for the forward elastic scattering cross section were found.

The experimental layout is shown in Fig. 1. A beam of protons scattered quasi-elastically from an internal Be target in the CERN Proton-synchrotron was used. Elastic p-p scatterings in the liquid hydrogen target were identified by measurements of the directions and momenta of the particles before and after the target. The incident proton beam, 5 mm in diameter

and generally containing about 300 particles per pulse, was defined by scintillation counters C_1, C_2 and C_3 and the scattered protons were detected by counters C_4 and C_5. The defining scintillator C_4 had a hole allowing unscattered particles to pass through without detection. The minimum scattering angles defined by this counter were 2.6, 1.5 and 1.0 mrad for the 10.1, the 19.3 and the 26.4 GeV/c runs, respectively. Scattering over the full azimuth could be detected up to 9 mrad at 10.1 GeV/c and up to 5 mrad at the other two energies. The maximum scattering angle accepted by the apparatus at 10.1 GeV/c was 23 mrad while at 19.3 and 26.4 GeV/c it was 14 mrad. The background trigger rate from unscattered particles was reduced by an anti-coincidence counter C_6 directly in the path of the beam. The coincidence signature used to trigger the spark chambers in the scattering runs was $1\ 2\ 3\ 4\ 5\ \bar{6}$.

Multiple scattering and background throughout the system were reduced to a very low level by transporting the beam in vacuum and by minimizing the thickness of scintillators, vacuum windows and spark chamber plates.

The positions of the incident and scattered protons were measured to about ± 0.3 mm by sonic spark chambers [2], S_1-S_5. Each spark chamber had two gaps, four piezo-electric transducers detecting the sound signals in each gap. The forty sonic times-of-flight were digitized in units of 0.1 μs [2] and registered by forty 25 MHz scalers. The time-of-flight information for each event, together with other data such as the number of beam particles leading up to a spark chamber trigger, were recorded on magnetic tape [3] in a time of about 160 ms. This time delay limited the rate of obtaining data generally to one event per synchrotron cycle so that more than 20,000 triggers could be registered in one day.

The spark positions and subsequently scattering angles, momenta and interaction points were calculated from the magnetic tape data using the CERN IBM 7090 computer. Calibration runs, using the coincidence trigger $1\ 2\ 3\ 5$ and an empty target, giving the mean positions of the unscattered beam in the spark chambers, were made at regular intervals and the scattering angles and momenta were obtained with reference to these mean positions.

For unscattered protons the angular resolution function of the system was found to fall to 10% in an angular interval of 0.15 mrad and the full width at half height of the distribution of the momentum difference between ingoing and outgoing protons was about 0.5%.

The high precision in angle determination made it possible to compute the point of interaction for scattering events to about ± 10 cm in longitudinal position at scattering angles greater than 1.5 mrad. The background associated with scattering in the scintillator and spark chamber material at each end of the hydrogen target was largely removed by rejecting events having interaction points clearly outside the space occupied by the liquid hydrogen. Background measurements using an empty dummy target were also performed. The residual background to be subtracted, at 19 GeV/c for example, was about 4% for elastic events between 2 and 3 mrad and less than 1% at larger angles.

Normally a 65 cm hydrogen target was used, in which case about 35% of the triggers were due to useful elastic events and about 12% to inelastic events. The remaining events were rejected for various reasons, either double sparks in a chamber (≈ 20%), or scattering from the spark chambers and scintillation counters near the hydrogen target (≈ 15%), or events outside the fiducial region in the trigger system (≈ 15%).

Absolute differential elastic scattering cross sections were obtained from the number of particles included within the elastic peaks in the momentum distribution of the scattered protons and the total number of beam particles. Uncertainties from inelastic contributions in the elastic momentum peaks were always less than 1%.

Figure 2 shows the elastic scattering angular distributions obtained corrected for absorption in the hydrogen (≈ 11%) and in detectors (≈ 1%) and for the bias due to multiple particle events (≈ -1%). The differential cross sections obtained at 19.3 GeV/c using a 20 cm long hydrogen target, for which the hydrogen absorption correction was 3.5%, were in good agreement with those obtained with the longer target. Various fits to the data, described below, are shown in Fig. 2. Substantial deviations of the

cross sections above the optical theorem value for pure diffraction scattering, $(d\sigma/d\Omega)_o = (k\sigma_{tot}/4\pi)^2$, are seen at the three momenta studied.

The differential cross sections were analyzed using two models. First, fits were made on the assumption of a complex spin independent scattering amplitude f_n using the relations

$$f_n = \left(\frac{\sigma_{tot}}{4\pi\hbar}\right)\left[\rho(t)\ \exp\left(\frac{1}{2}A_R t\right) + i\ \exp\left(\frac{1}{2}A_I t\right)\right] \tag{1}$$

$$f_c = \frac{-2e^2}{\beta c |t|}(1 + i\epsilon) \tag{2}$$

$$\epsilon = 0.0073 \ln \frac{0.0437}{t} \tag{3}$$

$$\frac{d\sigma}{d\Omega} = p^2 \left| f_n + f_c \right|^2 + \text{corrections} \tag{4}$$

in which $t = -2\bar{p}^2(1-\cos\bar{\theta}) \approx -p^2\theta^2$ is the square of the four-momentum transfer in $(GeV/c)^2$, β is the laboratory velocity and σ_{tot} is the strong interaction total cross section. For the very small values of t involved the electromagnetic form factor of the proton has been taken equal to unity. The expression for the Coulomb amplitude was taken from the discussion of Bethe [4] and contains a small imaginary part ϵ. The interference of the latter with the large imaginary nuclear amplitude is always small and contributes, for example at $t = -1.8\ 10^{-3}(GeV/c)^2$, 2.3% to $d\sigma/d\Omega$. At larger momentum transfers this contribution is even smaller.

In the evaluation the following simplifications were made $A_I = A_R = A$, and $\rho(t) = \rho$ independent of t. Corrections amounting to about 1% were made to take account of multiple scattering in the hydrogen target and the presence of small non-additive Coulomb terms [5].

In the second model the characteristic shapes of the angular distribution were attributed to spin dependence of the p-p interaction. Imaginary singlet-triplet spin amplitude fits were made using the amplitude term

$$f_n = i\left(\frac{\sigma_{tot}}{4\pi\hbar}\right)\left[\sqrt{\frac{3}{4}}\,\frac{(3 + \vec{\sigma}_1\cdot\vec{\sigma}_2)}{4}a_3\ \exp\left(\frac{1}{2}A_3 t\right) + \sqrt{\frac{1}{4}}\,\frac{(1 - \vec{\sigma}_1\cdot\vec{\sigma}_2)}{4}a_1\ \exp\left(\frac{1}{2}A_1 t\right)\right] \tag{5}$$

and the optical theorem constraint

$$\frac{3}{4} a_3 + \frac{1}{4} a_1 = 1 \qquad (6)$$

together with equations (2), (3) and (4). The exponential slopes A_1 and A_3 for the singlet and triplet states and the amplitude coefficients a_1 and a_3 were varied to fit the experimental points.

The results of the calculations are given in Table 1 and shown in Fig. 2. The fits found on the assumption of a real part are satisfactory, as shown by the χ^2 probabilities in Table 1. The parameter ρ varies from -0.43 to -0.32 between 10.1 and 26.4 GeV/c. Statistical errors in the differential cross sections contributed 3% to the error in ρ. A 2% uncertainty in the normalization of the differential measurements contributed 8% and the quoted error (Table 1) in σ_{tot} contributed 5%. The exponential slopes A, measured at the very small momentum transfer of this experiment are the same, within the uncertainties of the fit, as those found in previous measurements at larger $|t|$ by Foley et al [1].

On the other hand, the use of imaginary singlet-triplet spin amplitudes gave much poorer fits. The very steep rise of the angular distributions with decreasing momentum transfer appears to be characteristic of Coulomb interference and, as shown in Fig. 2, could not be reproduced by the constrained exponential fits.

On the basis of the good real part fits the experimental data can be explained by the presence of a real spin independent amplitude, 30-40% of the imaginary. It is also apparent that the angular dependence of the real part cannot be too different from that of the imaginary part.

A situation intermediate between the extreme models discussed, that is to say with different <u>complex</u> spin amplitudes, is so complicated that more information than simple scattering angular distributions is needed.

The data needed to find the p-p strong interaction total cross sections, σ_{tot}, used in the analyses were obtained piecemeal with the same beam and apparatus as were the differential cross sections. The transmission total cross section determined by the geometry of the trigger system, C_{12345},

was found by replacing the scintillator C_4 by one without a hole and by measuring the ratio of the counting rates 1 2 3 4 5 to 1 2 3 for both hydrogen and background runs. The contribution to σ_{tot} found in this way was, for example at 19.3 GeV/c, 35.3 mb out of 38.9 mb. The cross sections for inelastic and elastic events included within the normal triggering counter system were obtained from the counting rates found in the differential cross section runs.

To obtain the strong interaction total cross sections from the experimental data it is necessary to eliminate all contributions from electromagnetic interactions. The most important of these are ordinary Coulomb scattering and possible interference between the Coulomb and the strong interaction amplitudes. The former can be dealt with accurately but the latter is model dependent. Using the real amplitude fit described above it was found that the Coulomb interference contributed about 0.4 mb to the total cross sections. The σ_{tot} found after removal of this contribution are given in Table 1 and are the correct strong interaction total cross sections for the real part fits. It is worth noting that Coulomb interference contributions could be larger at lower energies and that the precise measurement of strong interaction total cross sections demands more detailed information than has been generally available in standard transmission measurements.

The best fit values of ρ, the ratio of real to imaginary forward scattering amplitudes, are plotted against the incident momentum in Fig. 3 together with values obtained from other recent experiments [6]. The trend shown below 1.5 GeV/c is taken from the discussion of Dowell et al [6]. The interesting qualitative features of Fig. 3 are the change of sign of ρ, from an attractive to a repulsive behaviour, at about 1.7 GeV/c and the large and rather constant value at momenta above 10 GeV/c. This change in character of the real part suggests a correlation with the momentum variation of the p-p total cross section, which exhibits a very rapid increase between 1 and 2 GeV/c followed by a slowly falling plateau. The positive real part may then be essentially different from the negative real part as the p-p interaction below the multiple meson production threshold is different from that above. Following these lines of thought it may be conjectured that the negative, repulsive real part will not decrease any more rapidly with energy than the

inelastic cross section and will remain different from zero at the very highest energies, provided that the inelastic processes remain in operation.

Dr. C.C. Ting made valuable contributions in the early stages of the experiment and Mr. S. Dahlgren helped in experimental runs.

We wish to thank the Proton-synchrotron Division for their whole hearted collaboration, especially Dr. J. Geibel who designed the beam and L. Mazzone and G. Coubra who were responsible for the liquid H_2 target.

We are grateful to F. Iselin, E. Långh and A. Maurer for their enthusiastic cooperation in designing and putting into operation the data transfer and recording equipment used in this experiment and to C.A. Ståhlbrandt, C. Sherwood and J. Goodchild for their development of the spark chamber circuitry. R. Donnet, K. Traub and M. Ferrat are thanked for the production of the spark chambers and associated equipment.

Useful conversations with Dr. L. van Hove and Dr. H. Pilkuhn and the constant support and interest of Dr. P. Preiswerk are gratefully acknowledged.

T A B L E I

Best fit values of the parameters in the Coulomb interference and in the singlet-triplet models

		10.11 GeV/c	19.33 GeV/c	26.42 GeV/c
COULOMB INTERFERENCE MODEL	ρ	-0.43 ± 0.043	-0.33 ± 0.033	-0.32 ± 0.033
	Λ (GeV/c^{-2})	10.4 ± 0.4	10.0 ± 0.2	10.2 ± 0.2
	χ^2 probability of best fit	50%	4%	85%
	σ_{total} (mb)	40.0 ± 0.3	38.9 ± 0.3	38.8 ± 0.3
SINGLET-TRIPLET MODEL	a_1	2.43 ± 0.05	2.22 ± 0.05	2.17 ± 0.05
	a_3	0.52 ∓ 0.02	0.59 ∓ 0.02	0.61 ∓ 0.02
	A_1 (GeV/c^{-2})	16 ± 1	12 ± 0.5	11 ± 0.5
	A_3 (GeV/c^{-2})	350 ± 50	300 ± 50	250 ± 50
	χ^2 probability of best fit	$< 10^{-6}$	$< 10^{-6}$	2%

REFERENCES

† Present address University of Bergen, Bergen, Norway.

†† University of Bern, now at University of California, Los Angeles, California, USA.

* Permanent address A.E.R.E., Harwell, Didcot, Berks., England.

** Present address Imperial College, London, England.

(1) W.M. Preston, R. Wilson and J.C. Street, Phys.Rev. 118, 579 (1959).

A.N. Diddens, E. Lillethun, G. Manning, A.E. Taylor, T.G. Walker and A.M. Wetherell, Phys.Rev.Letters 9, 108 (1962).

L.F. Kirillovn, V.A. Nikitin, A.A. Nomofilov, V.A. Sviridov, L.N. Strunov and M.G. Shafranova, Proc. Sienna Conf. on Elementary Particles (1963), Vol. 1, p. 593.

V.A. Bull and D.A. Garbutt, Phys.Rev. 130, 1182 (1963).

K.J. Foley, S.J. Lindenbaum, W.A. Love, S. Ozaki, J.J. Russell and L.C.L. Yuan, Phys.Rev.Letters 11, 425 (1963).

H. Eggstain and G. Kellner, Proc. Sienna Conf. on Elementary Particles (1963), Vol. 1, p. 598.

(2) G. Cocconi, A.N. Diddens, E. Lillethun, J. Pahl, A.C. Sherwood, J.P. Scanlon, C.A. Ståhlbrandt, C.C. Ting, J. Walters and A.M. Wetherell, Proc. Informal Meeting on Film-less Spark Chamber Techniques and Associated Computer Use, CERN 64-30 (1964), p. 183.

(3) F. Iselin, S. Långh, A. Maurer, P. Ponting and E. Schuller, Proc. Informal Meeting on Film-less Spark Chamber Techniques and Associated Computer Use, CERN 64-30 (1964), p. 211.

(4) H.A. Bethe, Annals of Physics 3, 190 (1958).

(5) N.N. Achasov and V.F. Pleshakov, Report T.F.-11 (1964). U.S.S.R. Academy of Sciences, Novosibirsk.

(6) J.D. Dowell, R.J. Homer, Q.H. Khan, W.K. McFarlane, J.S.C. McKee and A.W. O'Dell, Phys.Letters 12, 252 (1964).

K.J. Foley, R.S. Gilmore, R.S. Jones, S.J. Lindenbaum, W.A. Love, S. Ozaki, E.H. Willen, R. Yamada and L.C.L. Yuan, reported at Dubna Conference August 1964.

A.E. Taylor, A. Ashmore, W.S. Chapman, D.F. Falla, W.H. Range, D.B. Scott, A. Astbury, F. Capocci and T.G. Walker, Phys.Letters, to be published.

S.J. Lindenbaum, Summary Report at Dubna Conference August 1964.

L. Kirillova, L. Khristov, V. Nikitin, M. Shafranova, L. Strunov, V. Sviridov, Z. Korbel, L. Rob, P. Markov, Kh. Tchernev, T. Todorov and A. Zlateva, Phys.Letters 13, 93 (1964) and Dubna Report E-1820 (1964).

H. Lohrmann, H. Meyer and H. Winzeler, Phys.Letters 13, 78 (1964).

FIGURE CAPTIONS

(1) Experimental layout

(2) Proton-proton elastic scattering angular distributions at 10.1, 19.3 and 26.4 GeV/c.
Sections (a), (b) and (c) give the experimental cross sections plotted against scattering angle and show fits made using a complex spin independent amplitude.
In (d), (e) and (f) X is the difference between the experimental and Coulomb cross sections, normalized to the optical theorem value $(k\sigma_{tot}/4\pi)^2$.X is shown as a function of the square of the 4-momentum transfer t.
Attempts at singlet-triplet imaginary amplitude fits are shown.

(3) The ratio of the real and imaginary parts of the forward elastic scattering amplitude, ρ, as a function of momentum. The sources of the points are reference 6 and the first entry of reference 1. The error bars on the points of Foley et al are preliminary estimates.

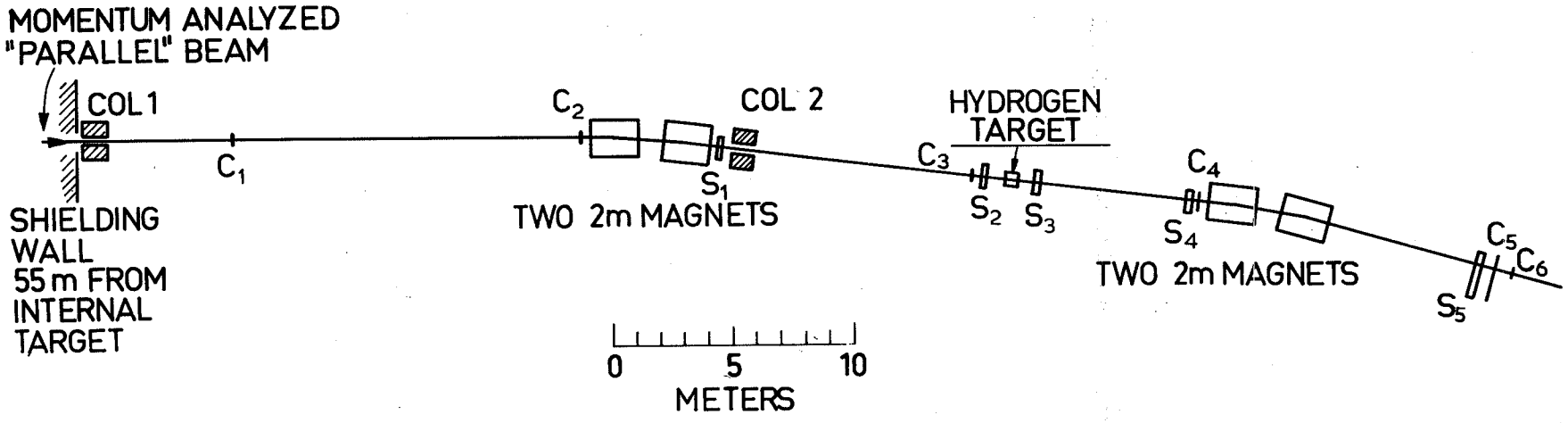

Fig.1

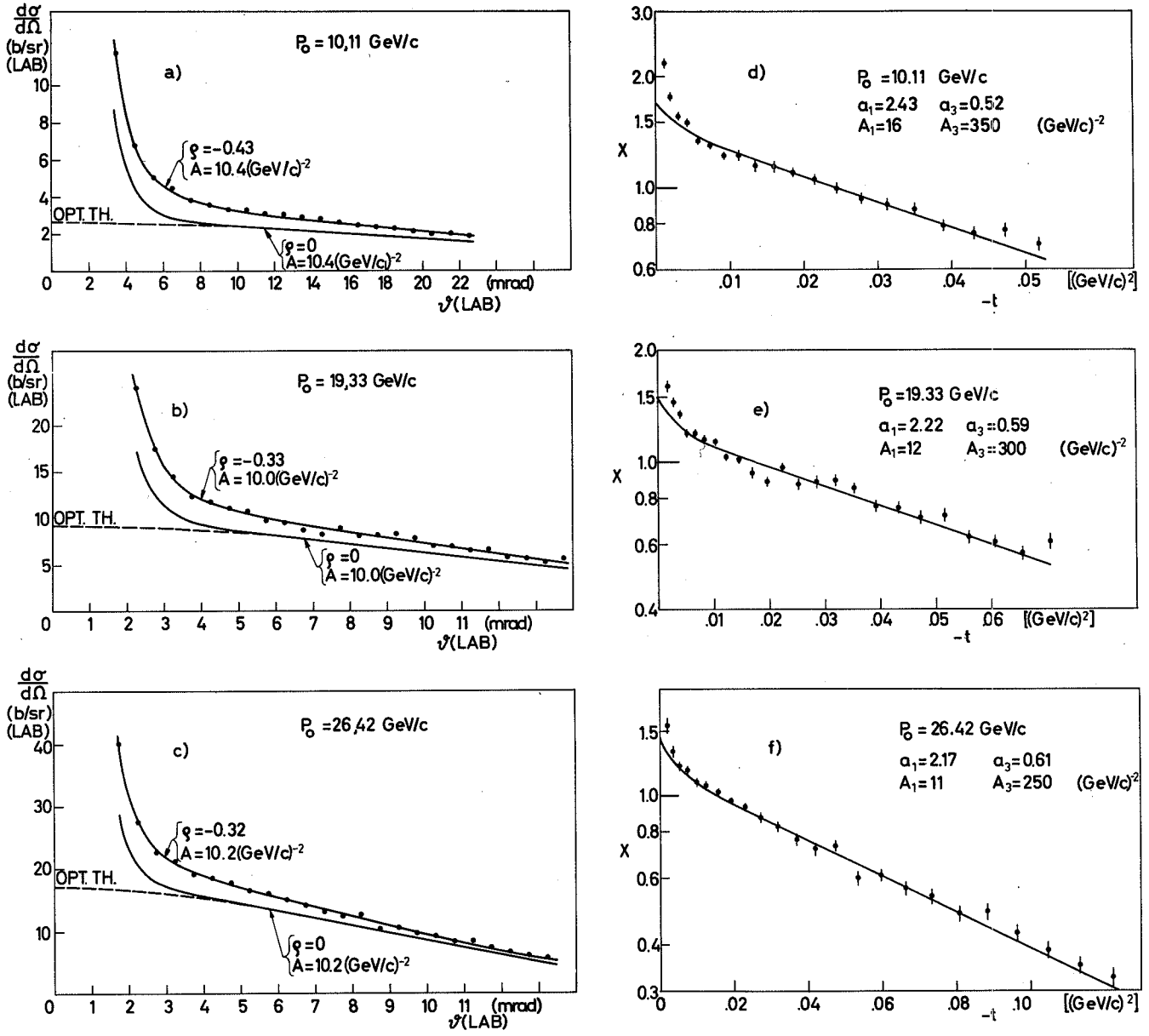

Fig.2

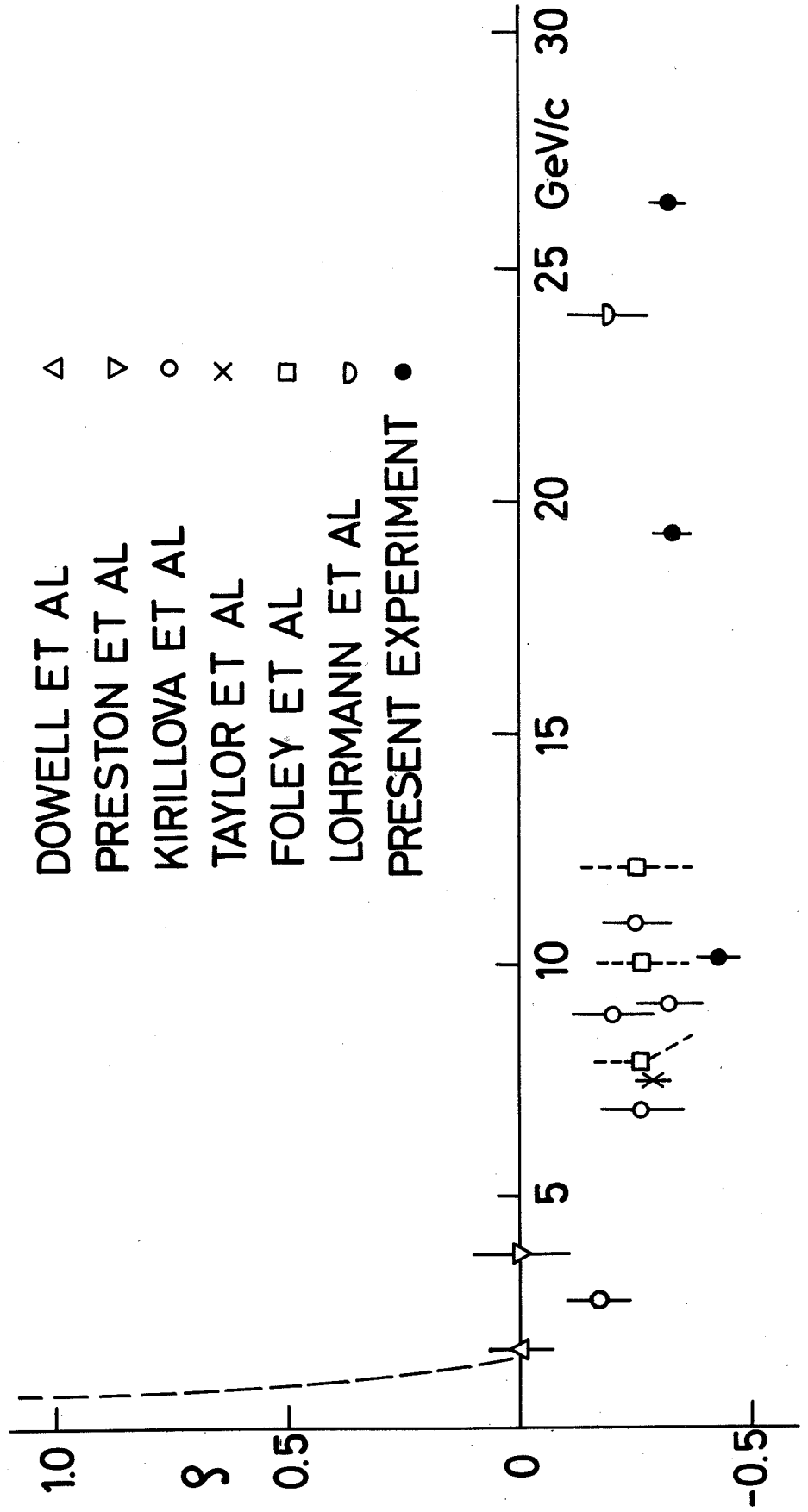
DOWELL ET AL
PRESTON ET AL
KIRILLOVA ET AL
TAYLOR ET AL
FOLEY ET AL
LOHRMANN ET AL
PRESENT EXPERIMENT
1.0
0.5
0
-0.5
5
10
15
20
25
30
GeV/c

Fig.3